

GLOBAL AND LOCAL LOSS SUPPRESSION IN THE UA9 CRYSTAL COLLIMATION EXPERIMENT*

S. Montesano, CERN, Geneva, Switzerland, and W. Scandale[#], CERN, Geneva, Switzerland, LAL, Orsay, France, and INFN, Roma 1, Italy, for the UA9 Collaboration

Abstract

UA9 was operated in the CERN-SPS for some years in view of investigating the feasibility of the halo collimation assisted by bent crystals. Silicon crystals 2 mm long with bending angles of about 150 μ rad are used as primary collimators. The crystal collimation process is obtained consistently through channeling with high efficiency. The loss profiles in the area of the crystal-collimator setup and in the downstream dispersion suppressor area show a steady reduction of slightly less than one order of magnitude at the onset of the channeling process. This result holds both for protons and for lead-ions. The corresponding loss map in the accelerator ring is accordingly reduced. These observations strongly support our expectation that the coherent deflection of the beam halo by a bent crystal should enhance the collimation efficiency in hadron colliders, such as LHC.

INTRODUCTION

In hadron colliders, such as the LHC, superconducting magnet technology and high-intensity beams are used to guarantee a large discovery potential. Halo particles surrounding the beam core may produce high-power loss. Multi-stage collimation systems should safely absorb them. The primary collimator is the first solid target that repeatedly intercepts the diffusive halo particles, imparting to them random angular kicks by multiple Coulomb scattering. Such a process brings them into the secondary collimators and the absorber. Due to the very low diffusion speed and to the very small impact parameter, the halo particles have a finite probability of being back-scattered in the vacuum pipe and of producing residual loss detrimental for the accelerator and for the experimental detectors. Many collimation stages favour the probability of promptly reabsorbing them and improve the collimation performance. In the four-stage LHC setup, a cleaning efficiency of 99.93% is routinely reached [1].

A bent crystal replacing the primary collimator should reduce by an order of magnitude the residual collimation leakage [2], [3]. The majority of the incoming particles are deflected during the first crystal traversal. Those that escape deflection will cross the crystal again and have an additional probability of being coherently deflected and absorbed in subsequent turns. This gives some advantage to crystal-assisted collimation process. The impact parameter with the secondary collimators and the absorber is considerably increased. Bent crystals being much shorter than primary amorphous collimators, the

accelerator impedance is to some extent reduced and the beam stability increased. Finally, particles trapped in the crystal planes have fewer encounters with the nuclei of the lattice resulting in a reduced probability of nuclear interactions, of diffractive proton scattering and, for ion beams, of fragmentation and electromagnetic dissociation events. As a consequence of this, crystal assisted collimation should enhance global and local loss suppression.

EXPERIMENTAL APPARATUS

Figure 1 shows the schematic layout of UA9 installed in the straight section 5 of the SPS [4]. Two stations at 90° phase advance and at large values of the horizontal beta function close to the quadrupoles QF1 and QF2, respectively, act as a two-stage horizontal collimation set up. The first station contains four crystals C1 to C4. Each of them, mounted on a mechanical goniometer, can be moved close to the beam core and oriented parallel to the halo particle trajectory thus acting as primary collimator. The second station located 60 m downstream contains a 60 cm long tungsten absorber (TAL) that can be moved towards the beam core to collect the deflected halo particles thus acting as secondary collimator.

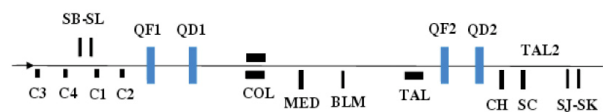


Figure 1: Schematic layout UA9.

About 40 m downstream of the crystals there is an LHC-type collimator (COL) made of two-sided copper jaws 1 m long that can be moved horizontally to precisely define the beam envelope and identify the beam orbit center. The collimator is also used to scan the deflected beam. The showers induced by the intercepted flux are seen by a beam loss monitor (BLM) downstream and give information about the deflecting angle and the channeling efficiency of the crystal. A Roman Pot is installed after the collimator: it comprises two horizontal axes with linear motors, each supporting a secondary vacuum vessel with a Medipix detector (MED) made of square 55 μ m pixels. The detector can be moved towards the pipe axis to intercept the deflected beam, thus providing an online image of the beam.

About 120 m downstream of the crystals the dispersion function increases to its maximal value. Limiting aperture devices (TAL2) are located there for optimal detection of the off-momentum halo escaping from the collimation

*Work supported by EuCARD program GA 227579, in "Collimators and Materials for high power beams" (Colmat-WP) and by LARP.

[#]walter.scandale@cern.ch

stations. The escape mechanism is inherent to the collimation process. Single diffractive events in the primary collimator may leave the trajectory unchanged and substantially reduce the energy of the incident particles, thereby preventing the secondary absorber from collecting them. Those particles have larger orbit deviations as the dispersion function increases. The deviation is maximal at the TAL2 position. In bent crystals, ionization energy loss and nuclear interactions are substantially reduced [5]. So should be the diffractive interactions and the population of self-generated off-momentum halo. One the main goal of UA9 is to measure the reduction of the loss rate close to the crystal and in the high-dispersion area the TAL2. In the latter position, two horizontally movable devices in the inner side of the SPS ring can intercept and evaluate the secondary halo population escaping collimation. A 10 cm long duralumin bar (SC) is used as a scraper and a BLM downstream is used to evaluate the incoming flux. A Cherenkov detector (CH) nearby can scan and count the intercepted flux. Scintillation counters such as SB and SL close to the crystals and SJ and SK close to TAL2 are used to detect local losses.

EXPERIMENTAL RESULTS

During UA9 runs, a single bunch of a few ns length and $10^9 - 10^{11}$ protons or Pb ions is stored in the SPS at 270 GeV. The lifetime is of one to 10 hours, depending on the selected distance of the primary crystal from the beam closed-orbit. The average amplitude growth of particle oscillations is smaller than 0.1 nm per turn.

The experimental procedures to test crystal collimation are discussed in Ref. [6]. Data referring to crystals C3 and C4 are reported hereafter.

Figure 2 shows the response of the proton beam loss monitor to an angular scan of crystal C4. The loss count is plotted as a function of the C4 orientation. The dashed line corresponds to the loss rate for amorphous orientations of the crystal to which the loss rate is normalized. The plot shows a minimum at 2140 μrad . For this orientation the fraction of beam halo deflected by the crystal in channeling states is maximal, the inelastic interactions in the crystal are minimal and the beam loss rate downstream of the crystal location decreases by a factor 10 with respect to the amorphous orientations. Such an angular scan is the optimal way to find the best orientation for channeling: simulations show that around the loss minimum the channeling efficiency varies slowly whilst the inelastic interaction probability varies very strongly. On the right of the loss minimum, there is a wide angular range of significant beam loss reduction due to volume reflection (VR) of halo particles in the crystal. Its width equals the crystal bend angle. In VR the particles thus perform a smaller number of passages through the crystal to reach the TAL aperture than for amorphous orientations. This reduces the total number of inelastic interaction losses in the crystal. The beam halo fraction escaping from the collimation area was estimated with the TAL2 devices.

Scans were made from the garage position to the beam edge. Figure 3 shows the dependence of the BLM count on the horizontal position of the SC jaw during two such scans made with C4 in amorphous (AM) and channeling (CH) orientations. The plot is made with protons. Particles intercepted behind the TAL shadow should have escaped from collimation with negative off-momentum values. Their population was reduced by a factor of at least 3 when rotating C4 from amorphous to channeling orientation.

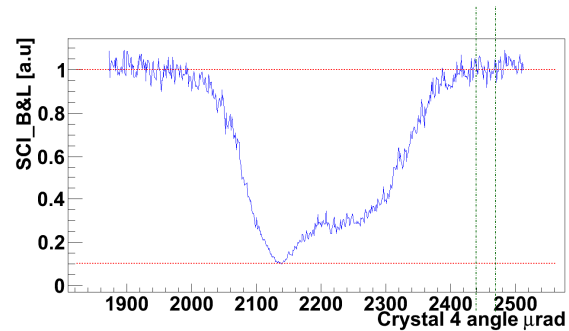


Figure 2: Angular scan of the crystal C4. The dashed line refers to amorphous orientation of the crystal.

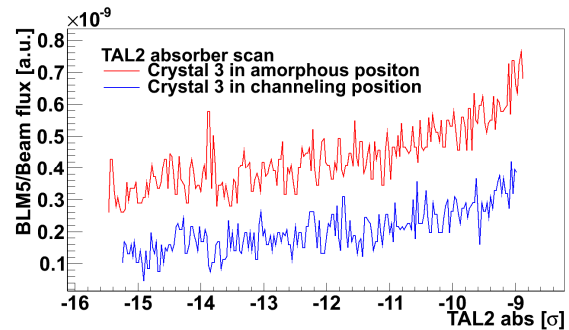


Figure 3: Dependence of beam loss monitor signal normalized to beam intensity on the horizontal position of the scraper (SC) in the high dispersion area behind the collimator-absorber. SC moves towards the beam periphery. CR3 is in amorphous (upper line in blue) or in channeling (lower line in red) orientation.

When using Pb ion beams, the channeling performance is about the same as for protons, except that ionization losses and nuclear interaction rates are larger. In a 2 mm long silicon crystal in amorphous orientation the mean energy loss is 1.05 MeV for protons and 6.59 GeV for Pb ions, corresponding to relative off-momentum $\delta_p = 8.7 \times 10^{-6}$ and $\delta_{pb} = -0.66 \times 10^{-3}$. The total cross-section for inelastic nuclear interactions and electromagnetic dissociation of Pb ion in silicon is 10 times larger than for protons. The attenuation length is 3.76 cm, thus about 5% of the Pb ions is lost per crystal traversal. Angular scans with Pb ions were thus expected to give a flatter response than with protons.

In Figure 4, the Pb ion beam halo fraction deflected by C4 in channeling states was measured by using a scan of the COL jaws [7]. Its value was found to be 70%.

In Figure 5 the loss reduction factor close to the crystal was 1.6 in VR and about 5 in channeling. A similar loss reduction factor is observed in the dispersive area.

For Pb ions, as for protons, there is a discrepancy between the experimental and simulation values of beam losses in channeling and VR orientations that may be due to surface imperfections, bad accounting of multi-turn halo population and of crystal miscut effects.

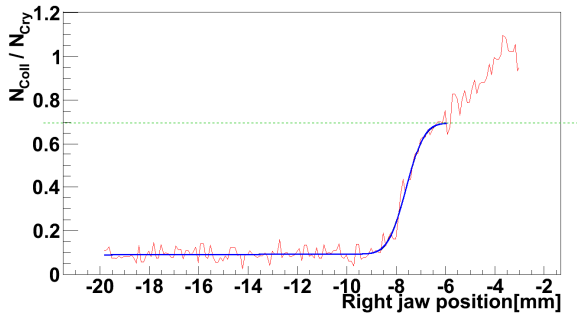


Figure 4: Channeling efficiency of CR4 with Pb-beams.

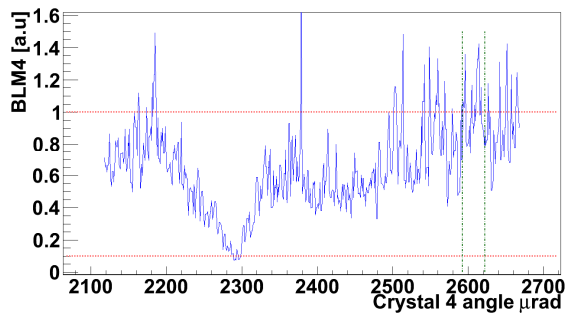


Figure 5: Angular scan of C4 with Pb-beams.

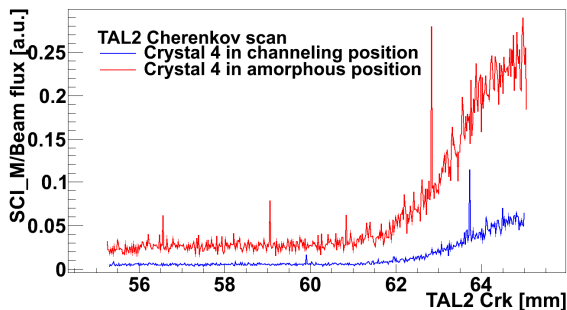


Figure 6: Scan of the dispersive area with Pb-beams.

The off-momentum Pb ion fraction generated in the collimation process was also measured by scanning the beam periphery in the TAL2 station with the SC jaw and the Cherenkov detector. A factor 5 reduction of the halo

population was observed in the absorber shadow when rotating the crystal from amorphous to channeling orientation. The result is shown in Figure 6

CONCLUSIONS

UA9 results demonstrate that crystal collimation can be routinely achieved for proton and Pb ion beams with a robust and well-reproducible procedure. Its performance is superior to that of a standard collimation setup with amorphous primary target. The improvement is threefold. In channeling orientation, the channeling efficiency is large, whilst the loss rate close to the crystal and the off-momentum halo escaping from collimation devices are strongly reduced. The performance is inferior to that predicted by simulations for reasons not yet clarified. However the experimental evidence strongly supports an extended test of crystal collimation in LHC. Strip or quasi-mosaic crystals have equivalent performance, although results not yet accounted show that strips are slightly better for Pb ions. The goniometer should be three times more accurate than in UA9, for faster and more reproducible orientation of the crystal at the higher energy in LHC. Other open issues are the crystal collimation performance at high intensity and halo flux rate, the robustness of the crystal and the absorber to high halo flux and the proper integration of the crystals in the existing LHC collimation system.

REFERENCES

- [1] R.W. Assmann et al., “Designing and Building a Collimation System for the High-Intensity LHC Beam”, PAC 03 Portland, Or, USA (2003).
- [2] R. W. Assmann, S. Redaelli, W. Scandale, “Optics study for a possible crystal-based collimation system for the LHC”, EPAC 06, Edinburgh (2006).
- [3] W. Scandale, “Crystal-based collimation in modern hadron colliders”, CERN-2009-04, p. 154 (2008).
- [4] W. Scandale et al, “The UA9 experimental layout”, submitted to JINST, Geneva (2011).
- [5] W. Scandale et al., Nucl. Inst. and Methods B 268 (2010) 2655-2659.
- [6] S. Montesano and W.Scandale for the UA9 Collaboration, “apparatus and experimental procedures to test crystal collimation”, these proceedings.
- [7] W.Scandale et al., Phys. Letters B 692 (2010) 78.